Emission properties of electrically pumped triangular shaped microlasers

Martina Hentschel,[1,*] **Qi Jie Wang,**[2,3] **Changling Yan,**[2,4] **Federico Capasso,**[2] **Tadataka Edamura,**[5] **and Hirofumi Kan**[5]

[1]*Max-Planck Institut für Physik komplexer Systeme, 01187 Dresden, Germany*
[2]*School of engineering and applied sciences, Harvard University, Cambridge, MA, 02138, USA*
[3]*Now with School of electrical and electronic engineering, Nanyang Technological University, 50 Nanyang Ave, 639798, Singapore*
[4]*Now with Changchun University of Science and Technology, Changchun, 130022, China*
[5]*Central research laboratory, Hamamatsu Photonics K.K., Hamamatsu 434-8601, Japan*
**martina@pks.mpg.de*

Abstract: We study the emission properties of electrically pumped triangular-shaped microlasers with rounded corners. We find no signs of directional emission for the relatively large cavities (dimension $\sim 100\mu$m) used in our experiments, in full agreement with ray simulation results. The broad emission characteristics that we observe can be fine-tuned by adjusting the resonator geometry as is verified through simulations which might prove useful for applications in optical devices.

OCIS codes: (140.3410) Laser resonators; (140.3945) Microcavities; (140.1540) Chaos.

References and links

1. K. J. Vahala, "Optical microcavities," Nature (London) **424**, 839 (2003).
2. J. Wiersig and M. Hentschel, "Combining Directional Light Output and Ultralow Loss in Deformed Microdisks," Phys. Rev. Lett. **100**, 033901 (2008).
3. C. Yan, Q. J. Wang, L. Diehl, M. Hentschel, J. Wiersig, N. Yu, C. Pflügl, F. Capasso, M. A. Belkin, T. Edamura, M. Yamanishi, and H. Kan, "Directional emission and universal far-field behavior from semiconductor lasers with limaçon shaped microcavity," Appl. Phys. Lett. **94**, 251101 (2009).
4. Q. J. Wang, C. Yan, L. Diehl, M. Hentschel, J. Wiersig, N. Yu, C. Pflügl, M. A. Belkin, T. Edamura, M. Yamanishi, H. Kan, and F. Capasso, "Deformed microcavity quantum cascade lasers with directional emission," N. J. Phys. **11**, 125018 (2009) and References therein.
5. J. Wiersig and M. Hentschel, "Unidirectional light emission from high-Q modes in optical microcavities," Phys. Rev. A **73**, 031802 (2006).
6. G. D. Chern, H. E. Tureci, A. Douglas Stone, R. K. Chang, M. Kneissl, and N. M. Johnson, "Unidirectional lasing from InGaN multiple-quantum-well spiral-shaped micropillars," Appl. Phys. Lett. **83**, 1710–1712 (2003) was the first reference on this topic, see also Refs. [2-6] in Ref. [8] below.
7. R. Audet, M. A. Belkin, J. A. Fan, B. G. Lee, K. Lin, and F. Capasso, "Single-mode laser action in quantum cascade lasers with spiral-shaped chaotic resonators," Appl. Phys. Lett. **91**, 131106 (2007).
8. M. Hentschel, T.-Y. Kwon, M. A. Belkin, R. Audet, and F. Capasso, "Angular emission characteristics of quantum cascade spiral microlasers," Opt. Express **17**, 10335–10343 (2009).
9. M. Hentschel and T.-Y. Kwon, "Designing and understanding directional emission from spiral microlasers," Opt. Lett. **34**, 163–165 (2009).
10. M. S. Kurdoglyan, S.-Y. Lee, S. Rim, and Ch.-M. Kim, "Unidirectional lasing from a microcavity with a rounded isosceles triangle shape," Opt. Lett. **29**, 2758–2760 (2004).
11. N. Yu, J. Fan, Q. J. Wang, C. Pflügl, L. Diehl, T. Edamura, M. Yamanishi, H. Kan, and F. Capasso, "Small-divergence semiconductor lasers by plasmonic collimation," Nat. Photonics **2**, 564–570 (2008).
12. H. G. L. Schwefel, N. B. Rex, H. E. Tureci, R. K. Chang, A. D. Stone, T. Ben-Messaoud, and J. Zyss, "Dramatic shape sensitivity of directional emission patterns from similarly deformed cylindrical polymer lasers," J. Opt. Soc. Am. B **21**, 923–934 (2004).

#127686 - $15.00 USD Received 27 Apr 2010; revised 17 Jun 2010; accepted 24 Jun 2010; published 21 Jul 2010

13. T. Tanaka, M. Hentschel, T. Fukushima, and T. Harayama, "Classical Phase Space Revealed by Coherent Light," Phys. Rev. Lett. **98**, 033902 (2007).

1. Introduction

Optical microcavities [1] such as microlasers with unidirectional emission properties have received growing interest during the past years. It is driven by a strong demand from the application side, namely to have the very useful properties of Fabry-Perot lasers available in devices that are only slightly larger in size than the wavelength of light. Miniaturization of the Fabry-Perot mechanism to such tiny scales fails because of shortcomings in the fabrication of the laser facets and the needed mirrors. Therefore, alternative ideas and mechanisms are needed in order to pursue the downscaling of optical and optoelectronic devices, thereby keeping both the relatively directional emission properties and the high-quality factors of the Fabry-Perot lasing modes.

A number of different mechanisms and resonator shapes have been employed to yield directional emission properties from modes with high quality factors. The most recent example are microlasers of limaçon shape [2–4] that show a robust and universal far-field pattern with a pronounced directionality especially for the case of TE-polarized light. Another possibility is to use the hybridization of modes at avoided resonance crossings, e.g. in circular cavities with an air hole (annular geometry) [5]. Earlier developments used microlasers of spiral shape and found directional emission from the so-called notch [6]. However, not all spiral microlasers were found to possess directional output characteristics [7], and pumping along the boundary was found to be a crucial prerequisite [6, 8, 9].

In the present Letter we discuss the emission properties of microlasers of triangular shape. Similar to the case of spiral-shaped microlasers, directional emission was reported in some occasions [10] but could not be confirmed in the triangular cavities used in our experiments, nor in the ray simulation data that we also report here. In fact, we find good agreement between our experimental results and the accompanying ray model simulations. The reason might lie in the different sizes of the devices investigated: The numerical simulations performed in Ref. [10] investigated a regime where the ratio of wavelength to cavity size was considerably larger than in the present case that is closer to the ray limit.

2. Device structure and fabrication

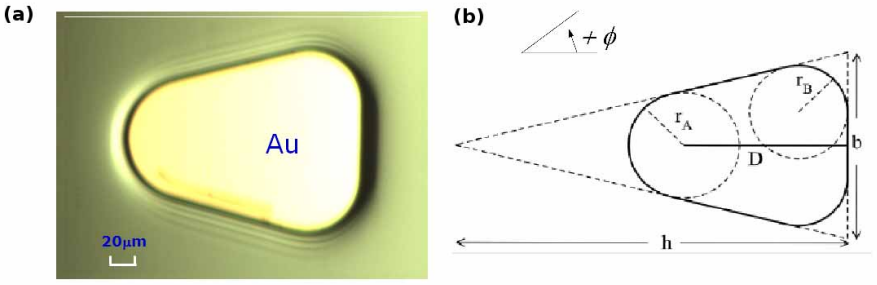

Fig. 1. (a) Micrograph of an experimental structure. (b) Schematics of the triangular cavity geometry. The parameters used in the experiment are $D = 150\mu$m, $b = 180\mu$m, $h = 360\mu$m, $r_A = 51\mu$m, $r_B = 45\mu$m, similar to those used in Ref. [10]. The far-field angle ϕ is indicated on the right.

#127686 - $15.00 USD Received 27 Apr 2010; revised 17 Jun 2010; accepted 24 Jun 2010; published 21 Jul 2010

In this work, we used electrically pumped quantum cascade lasers (QCLs) as an example to fabricate microcavity lasers. The electrical pumping scheme requires a relatively large top surface area (dimension $\sim 100\mu$m) for electric wire bonding that defines the comparatively large size of our cavities. QCLs were processed into triangular-shaped structures, see Fig. 1, with different deformation parameters D, b, r_A, r_B and h. The QCL material is the same as the one used in [4] designed at an emission wavelength of $\lambda \sim 10\mu$m. It is based on lattice-matched $Ga_{0.47}In_{0.53}As/Al_{0.48}In_{0.52}As$ heterostructures grown on top of an InP substrate. The active region consisting of 35 periodic stages has a thickness of $\sim 2\mu m$. The active region is sandwiched between two 520 nm-thick n-doped InGaAs layers followed by two 3.5 μm-thick n-doped (1×10^{17} cm^{-3}) epitaxial InP cladding layers. A 0.5 μm-thick n-doped (5×10^{18} cm^{-3}) InP layer is deposited on the top of the cladding layer, followed by a 10 nm highly doped (1×10^{19} cm^{-3}) InP contact layer.

Standard photolithography was used to define the contour of the laser and the structure was etched through the gain medium with a depth of $\sim 12\mu$m using inductively coupled plasma reactive ion etching to obtain vertical and smooth sidewalls. The sidewall of the etched device has a roughness of about 300 nm and is similar to that of the limaçon QCLs in [4], where a three-dimensional scanning electron microscope (SEM) image of the sidewall was shown. The active region covers the whole device area of QCLs, see Fig. 1(a). Then, the top and bottom metal contacts Ti/Au (10nm/200nm) were deposited by using electron-beam evaporation. The devices were then soldered with indium to copper heat sinks and wire bonded for testing.

A microscope picture of a fabricated cavity with $D = 150\mu$m [D is the characteristic size of the cavity, defined as the length between the bottom and the center of the left circle, see Fig. 1(b)], is shown in Fig. 1(a). All the other parameters that are needed to characterize the shape of the cavity are displayed in the schematic of the geometry of the cavity in Fig. 1(b).

3. Device characterization and analysis

The processed triangular QCLs were electric pumped and tested in pulsed mode at room temperature with 125-ns current pulses at 80-kHz repetition rate. The emission spectrum of the device in Fig. 1(a) measured with a Fourier Transform Infrared Spectrometer at a pump current of $1.1\times I_{th}$ was shown in Figs. 2(a), exhibiting a single mode emission near $\lambda \sim 10\mu$m. The laser operates in single mode at a pump current up to $1.25\times I_{th}$. At higher pump currents, more optical modes with complex spectral features are shown. To understand the origin of these modes, an in-depth investigation on the mode distributions inside the cavity is necessary, which is the objective of our future work.

Figures 2(b) shows the light output power versus current characteristics of our triangular QCL at room temperature. Light output power was measured with a calibrated thermopile detector and a polished metallic tube to collect the laser output. A peak output power of $\sim$ 2mW, a threshold current density of $\sim$ 2.5kA/cm^2, and a slope efficiency of $\sim$ 6 mW/A were obtained for this device. The threshold current of the triangular QCL is higher than $\sim$ 2.0kA/cm^2 of the limaçon QCLs fabricated with the same material [4], because limaçon cavity keeps high-Q whispering gallery modes. Although it is difficult to calculate Q-factor through ray simulations, experimental measurements on the gain coefficient, threshold current density and waveguide losses [4] suggest an estimated Q factor of $\sim$1000 for this triangular microcavity QCL, as compared to a value of $\sim$1250 for the limaçon QCL [4]. The slope efficiency of the device is lower than $\sim$ 12 mW/A of the limaçon QCLs, due to the inefficient light output coupling from the triangular QCLs.

#127686 - $15.00 USD Received 27 Apr 2010; revised 17 Jun 2010; accepted 24 Jun 2010; published 21 Jul 2010

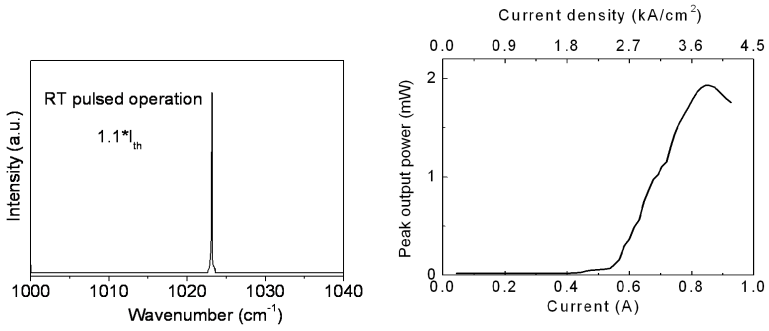

Fig. 2. (a) Spectrum of the lasing cavity at 11% (top) above the lasing threshold current. The emission wavelength is $\sim 10\mu$m in pulsed mode operation at room temperature. (b) Optical output power versus pump current measured at far-field angle $\phi = 0^o$ as a function of the pump current. The onset of lasing beyond a threshold current of about 0.53 A is clearly visible.

4. Far-field characteristics of triangular QCLs

Lateral far-field profiles of our devices were measured with a resolution of 0.5^o using a setup described in Ref. [11]. The device is mounted at the center of a rotation stage and a mid-infrared mercury-cadmium telluride detector is placed ~ 20 cm away to measure the output of the laser. The measured far-field patterns are shown in Fig. 3(a) for two different pumping currents of 750 mA and 870 mA, indicated by the black and red line, respectively, for the device in Fig. 1(a). Evidently, no characteristics of directional emission are visible, although the light is emitted predominantly to one side, namely to the sharper side of the triangular cavity. Further increase of the pump current increases the emission area into which the light is emitted, we believe this is due to the existence of other modes at high pumping currents which have slightly different far-field patterns. The experimentally observed far-field pattern at 870 mA is compared to the ray-simulation result in Fig. 3(b). Good agreement, up to a symmetry offset, between the two is displayed. The slight difference on the flat side of the triangular device (far-field angle 0 degree) is most likely due to the unavoidable sidewall surface scattering which broadens the measured far-field pattern.

Note that in Ref. [10] the emission was actually seen to originate from the flat side of the triangular QCLs, whereas we find the light to originate from the opposite, namely the sharper, side of the triangular cavity. We discuss a possible origin of these differences below.

5. Ray simulation results

The far-field emission patterns in the plane perpendicular to the QCL growth direction were calculated with ray optics simulations in a so-called Fresnel billiards [2, 12, 13] using an effective index of refraction $n = 3.2$. The simulations were carried out by starting a set of 25000 rays with initial conditions (specified by the polar angle and the ray's angle of incidence at the cavity boundary) that uniformly covered all possible values (i.e., the full "phase space"). The rays were started with unit intensity and propagated following the laws of specular reflection and using Fresnel laws (see Refs. [2, 12, 13] for details). Light escaping the cavity according to Snell's and Fresnel's law was collected after passing through a transient regime, i.e. after

#127686 - $15.00 USD Received 27 Apr 2010; revised 17 Jun 2010; accepted 24 Jun 2010; published 21 Jul 2010

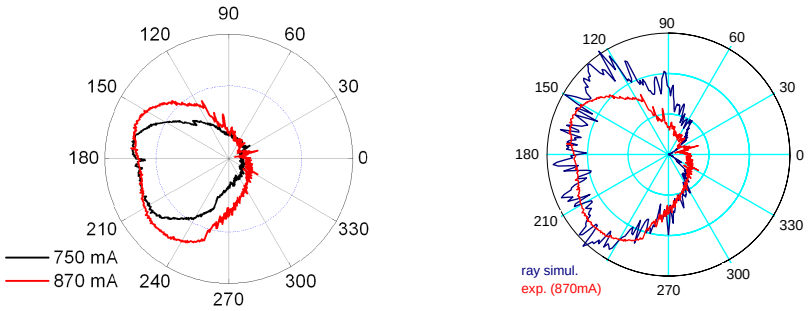

Fig. 3. (a) Far-field characteristics of triangular QCLs for two different pump currents. The black (red) line is for pumping current 750 mA (870 mA). Light is predominantly emitted towards the sharper side of the triangular structure. The axial symmetry of the cavity is seen to be slightly imperfect but very simlar for both pump currents. Both far-field intensity profiles are normalized to their maximum values. (b) Comparison of experimental and ray-simulation data, both normalized.

reaching a regime characterized by an exponential decay of the total intensity inside the cavity, and collected as the far-field emission characteristics. It was subsequently smoothed over two bins, and the results are shown in Fig. 4. As the character of (most of) the ray trajectories is chaotic, no simple, regularly shaped orbits can be identified to yield the observed far-field pattern. Rather, the far-field pattern is determined by the path that the rays take to escape the cavity that in turn is related to the so-called unstable manifold, see Ref. [2, 12, 13] for details.

The calculated far-field patterns (FFP) are shown in Fig. 4 for four slightly different geometries that are indicated to the left of each FFP panel. The geometry in Fig. 4(a) is exactly the one used in experiment. As ray optics corresponds to the limit of the wavelength $\lambda \to 0$, there exists no inherent characteristic length scale, and the resonator geometry is only defined up to an arbitrary length scale, that, for example, can be taken to be the length D. We point out that the radius r_A and D cannot be chosen independently, they are related via [here, α is half of the smallest angle of the dashed triangle shown in Fig. 1(b)] $r_A = (h-D)\sin\alpha = (h-D)\sin\left[\arctan(b/2h)\right]$.

6. Discussion and Conclusion

We have studied the far-field emission characteristics of triangular shaped QCL microcavities in experiments and through ray simulations. Experiment and calculated results are in very reasonable agreement and indicate that, as in many experiments accompanied by theoretical investigations before [2, 4, 8, 12, 13], the unstable manifold determines the far-field pattern. We find, contrary to the results reported in Ref. [10], no directional output from triangular microlasers. One possible explanation might be the excitation of qualitatively different lasing modes whose specific resonance properties lead to different far-field patterns. The fact that both experiments were conducted in very different nkD (n is the refractive index and k is the vacuum wavenumber) regimes ($28 < nkD < 30$ in Ref. [10] vs. $nkD \sim 300$ in the present study) supports this argumentation: The present study is, in comparison to the one in Ref. [10], closer to the ray limit (small wavelength, large nkD) and we found indeed reasonable agreement between the experimental results and ray-picture simulations. The results obtained in Ref. [10] refer to the behavior of a triangular cavity towards the wave limit and their deviation from the results reported here indicates the break-down of the validity of the ray model. Whereas this breakdown is not at all unexpected, there are a number of cases (see, e.g., Ref. [2]) where agreement with (naive) ray-model simulations was observed deep into the wave regime, in contrast to the

#127686 - $15.00 USD Received 27 Apr 2010; revised 17 Jun 2010; accepted 24 Jun 2010; published 21 Jul 2010

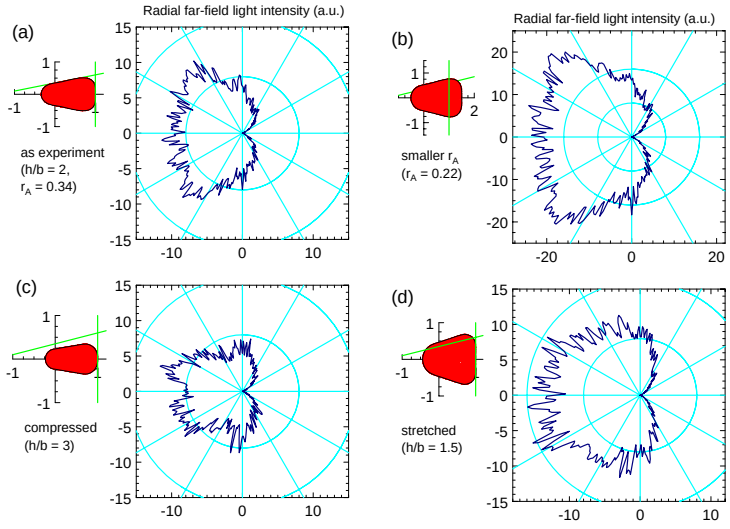

Fig. 4. Ray-simulation result for the radial far-field light intensity distribution for triangular cavities (arbitrary, but normalized units). The geometry in panel (a) is that used in the experiment, see also Fig. 1(b). The green lines mark the border of this "master" device and are repeated as a guide to the eye in the other panels. In panels (b-d), we study the influence of fabrication imperfections on the far-field pattern. A smaller radius r_A, panel (b), increases the overall far-field intensity since light emerges from this side of the cavity and the more easily the smaller the radius of curvature is. In panel (c) and (d), we show the results for vertically compressed and stretched structures, respectively. Lobes are somewhat more prominent in the compressed resonator shape, but all four geometries fully show the characteristics of the experimental result: A more or less homogeneous light output into about one third (120^o) of the resonator plane.

situation observed in Ref. [10].

Although the triangular cavities in the present study show a broad, rather than a directional, light output in the far field that covers more than one third of the resonator plane, we point out that ray-simulation results presented in Fig. 4 indicate that slight variations in the resonator geometry may allow to fine-tune the light output to be almost homogeneous, cf. Fig. 4(a), or to develop a lobed structure, cf. Fig. 4(c). Furthermore, variation of the radius of curvature at the three "corners" adjusts the light confinement and allows one to tune the overall light intensity in the far field. In occasions where directional light emission is not the primary goal, all these properties might be useful in the development of optical devices.

Acknowledgements

Martina Hentschel gratefully acknowledges support by the German Research Foundation (DFG) within the DFG Emmy-Noether Programme and the DFG research group 760. The Harvard authors acknowledge financial support from the Air Force Office Scientific Research (AFOSR). Device fabrication was carried out at the Center for Nanoscale Systems (CNS) at Harvard University, a member of the National Nanotechnology Infrastructure Network.

#127686 - $15.00 USD Received 27 Apr 2010; revised 17 Jun 2010; accepted 24 Jun 2010; published 21 Jul 2010